ELSEVIER

Synthetic Metals 132 (2003) 297–308

SYNTHETIC METALS

www.elsevier.com/locate/synmet

Photo-physical and lasing characterization of neat films of 4-methyl-TPD and of an alternating copolymer of 4-methyl-TPD with MEH–PPV

R. Philip[a,1], W. Holzer[a], A. Penzkofer[a,*], H. Tillmann[b], H.-H. Hörhold[b]

[a]*Institut II—Experimentelle und Angewandte Physik, Universität Regensburg, Universitatsstrasse 31, D-93040 Regensburg, Germany*

[b]*Institut für Organische Chemie and Makromolekulare Chemie der Universität Jena, Humboldtstrasse 10, D-07743 Jena, Germany*

Received 10 July 2002; accepted 7 October 2002

Abstract

Wave-guided traveling wave lasing, i.e. amplification of spontaneous emission in a waveguide, is studied on neat films of the triphenylamine dimer 4-methyl-TPD (*N*,*N*′-bis(4-methylphenyl)-*N*,*N*′-diphenyl-benzidine) and an alternating copolymer with MEH–PPV assigned as TPD(4M)–MEH–P–PPV. The solution processable polymer has been prepared via the polycondensation route. Laser action is achieved by transversally pumping neat films on glass substrates with picosecond excitation pulses (wavelength 347.15 nm, duration 35 ps). Lasing occurs around 422 nm for 4-methyl-TPD and around 544 nm for TPD(4M)–MEH–P–PPV. Below laser threshold leaky mode emission into the substrate along the film/surface interface is reported for 4-methyl-TPD. The optical constants (absorption spectra and refractive index spectra), the absorption cross-section spectra, fluorescence quantum distributions, fluorescence quantum yields, and fluorescence lifetimes of the samples are determined for photo-physical characterization. The laser performance and the photo-physical parameters of 4-methyl-TPD are compared with the molecule 3-methyl-TPD and the non-conjugated polymer poly-TPD(4M)–DPX which is built up of 4-methyl-TPD and α,α′-diphenylxylylene units. The parameters of TPD(4M)–MEH–P–PPV are compared with the parameters of TPD(4M)–MEH–PPV another alternating copolymer of 4-methyl-TPD with MEH–PPV. The synthesis details for TPD(4M)–MEH–PPV and TPD(4M)–MEH–P–PPV are given.

© 2002 Elsevier Science B.V. All rights reserved.

Keywords: Luminescent polymers; Wave-guided amplified spontaneous emission; Wave-guided traveling wave laser action; Mirror-less lasing; Leaky mode emission; Optical constants; Absorption behaviour; Fluorescence behaviour; Triphenylamine dimers; TPD; MEH–PPV

1. Introduction

The synthesis of laser active luminescent polymers and the development of polymer laser devices is an active field of research (for reviews see [1–7,8]). Laser action (including wave-guided traveling wave laser action) was achieved for various poly-phenylenevinylenes (PPVs) [1,2,5,9–16], poly-phenylene-ethynylenes (PPEs) [17], ladder-type poly-*para*-phenylenes (PPP) [3,18], polyfluorenes (PFs) [19,20], poly-phenylacethylenes (PPAs) [5,21], poly-arylene-vinylenes (PAVs) [22–26], poly-thiophenes (PTs) [27], triphenylamine (TPA)-based conjugated polymers [28,29], and triphenylamine dimer (TPD)-based conjugated and non-conjugated polymers [30–32]. Generally, no laser action is achieved for neat films of conventional organic laser dyes since molecular aggregation occurs and the fluorescence efficiency is strongly reduced [33–35]. Recently, laser action (optically initiated amplification of spontaneous emission) was achieved for neat films of the electrically active triphenylamine dimer 3-methyl-TPD [36] and of several spiro-type light-emitting molecules [37,38].

In this paper, wave-guided traveling wave lasing of neat films of low molecular *N*,*N*'-bis(4-methylphenyl)-*N*,*N*′-diphenyl-benzidine (4-methyl-TPD) and of a high molecular copolymer with phenyl-substituted MEH–PPV named TPD(4M)–MEH–P–PPV is reported. The obtained results are compared with previous studies on *N*,*N*′-bis(3-methylphenyl)-*N*,*N*'-diphenyl-benzidine (3-methyl-TPD) [36], poly-TPD(4M)–DPX [32], and on TPD(4M)–MEH–PPV [32]. It

* Corresponding author. Tel.: +49-941-943-2107; fax: +49-941-943-2754.
E-mail address: alfons.penzkofer@physik.uni-regensburg.de (A. Penzkofer).

[1] Present Address: Raman Research Institute, C.V. Raman Avenue, Sadashivanagar, Bangalore 560080, India.

0379-6779/02/$ – see front matter © 2002 Elsevier Science B.V. All rights reserved.
PII: S0379-6779(02)00499-X

should be noted that traveling wave lasing abbreviated by TWL [39–41], amplified spontaneous emission abbreviated by ASE [42,43], lasing without feedback [44] or mirror-less lasing [5,44,45], and laser generation or laser generator operation [46] describe the same effect of amplification of fluorescence light by stimulated emission and may be used synonymously. Here, traveling wave lasing is preferentially used to express the wave propagation without interfering feedback (no standing wave pattern formation). Besides lasing studies, some photo-physical parameters of 4-methyl-TPD and TPD(4M)–MEH–P–PPV (optical constants, absorption cross-section spectra, fluorescence quantum distributions, fluorescence quantum yields, and fluorescence lifetimes) are determined and compared with the parameters of 3-methyl-TPD [36], poly-TPD(4M)–DPX [32], and TPD(4M)–MEH–PPV [32]. The synthesis of TPD(4M)–MEH–PPV and TPD(4M)–MEH–P–PPV is described in Appendix A, and a detailed material characterization is given there.

2. Experimental

The structural formulae of the molecules 3-methyl-TPD and 4-methyl-TPD and of the conjugated copolymers TPD(4M)–MEH–PPV and TPD(4M)–MEH–P–PPV are shown in Fig. 1, together with the non-conjugated poly-TPD(4M)–DPX. 3-Methyl-TPD and 4-methyl-TPD were purchased from SynTec, 06766 Wolfen, Germany. The synthesis of the conjugated polymers TPD(4M)–MEH–PPV and TPD(4M)–MEH–P–PPV was only roughly described in [31], and is now given in more detail in Appendix A. Thin films on glass substrates were formed by dissolving the materials in toluene (20 mg material per 1 cm^3 toluene) and spin-coating the solutions on the substrates. The solvent evaporated before film usage. Neat films and solutions in dioxane of 4-methyl-TPD and TPD(4M)–MEH–P–PPV were investigated for spectroscopic characterization.

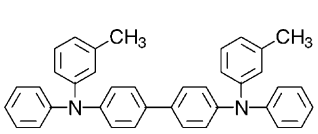

TPD(3M)

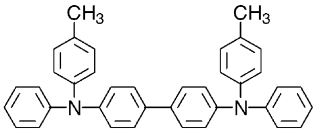

TPD(4M)

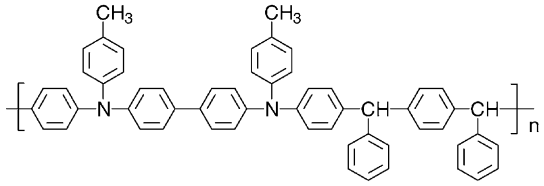

Poly-TPD(4M)-DPX

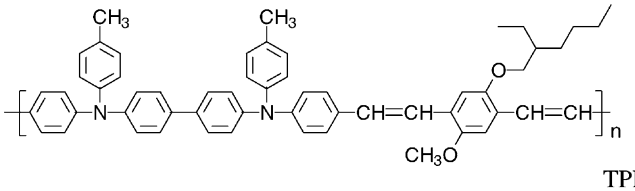

TPD(4M)-MEH-PPV

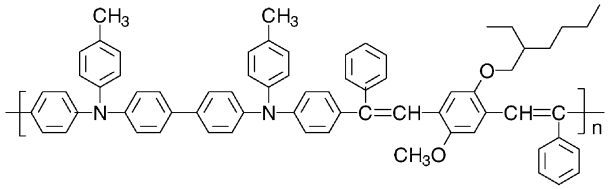

TPD(4M)-MEH-P-PPV

Fig. 1. Structural formulae of 3-methyl-TPD, 4-methyl-TPD, the non-conjugated polymer poly-TPD(4M)–DPX and the conjugated polymers TPD(4M)–MEH–PPV, and TPD(4M)–MEH–P–PPV (short names). Full names and sum formulae of the repeat units are listed as follows. 3-Methyl-TPD: *N*,*N*′-bis(3-methylphenyl)-*N*,*N*′-diphenyl benzidine ($C_{38}H_{32}N_2$). 4-Methyl-TPD: *N*,*N*′-bis(4-methylphenyl)-*N*,*N*′-diphenyl benzidine ($C_{38}H_{32}N_2$). Poly-TPD(4M)–DPX: poly[(4-methylphenyl)imino-4,4′-diphenylene-(4-methyl-phenyl)imino-1,4-phenylene-phenylmethylene-1,4-phenylene-phenylmethylene-1,4-phenylene] ($[C_{58}H_{46}N_2]_n$). TPD(4M)–MEH–PPV: poly[(4-methylphenyl)imino-4,4′-diphenylene-(4-methyl-phenyl)imino-1,4-phenylene-ethenylene-2-methoxy-5-(2-ethylhexyloxy)-1,4-phenylene-ethenylene-1,4-phenylene] ($[C_{57}H_{56}N_2O_2]_n$). TPD(4M)–MEH–P–PPV: poly[(4-methylphenyl)imino-4,4′-diphenylene-(4-methyl-phenyl)imino-1,4-phenylene-1-phenyl-ethenylene-2-methoxy-5-(2-ethylhexyloxy)-1,4-phenylene-2-phenyl-ethenylene-1,4-phenylene] ($[C_{69}H_{64}N_2O_2]_n$).

The technique of optical constants measurement of thin films by reflectance and transmittance measurements has been described previously [47,48]. The experimental arrangement for the measurements is shown there. The technique of fluorescence quantum distribution and fluorescence quantum yield measurement is described in [49] and the experimental arrangement is shown there. As reference fluorescence solution we used quinine sulfate dihydrate (from Aldrich) in 1N aqueous H_2SO_4 (fluorescence quantum efficiency $\phi(C) = 0.546/[1 + 14.5C]$ at 25 °C, where C is the dye concentration (mol dm^{-3}) [50]) for 4-methyl-TPD, and coumarin 314T in ethanol for TPD(4M)–MEH–P–PPV (fluorescence quantum yield $\phi = 0.87$ (technical data sheet of Kodak)). The fluorescence lifetime measurements have been carried out by preparing extremely thin films (no waveguiding, no amplified spontaneous emission), by exciting the samples with picosecond light pulses and detecting the fluorescence signal with a fast micro-channel-plate photomultiplier (Hamamatsu type R1564U-01) and a fast real-time digital oscilloscope (LeCroy type 9362).

The traveling wave lasing studies are carried out by transversally exciting the samples with single picosecond frequency-doubled pulses of an active and passive mode-locked ruby laser (pulse duration $\Delta t_L \approx 35$ ps, wavelength $\Delta\lambda_L = 347.15$ nm, pulse energy up to $W_L = 1$ mJ). The experimental procedure and the experimental setup have been described previously in [2,24].

3. Results

3.1. Optical and spectroscopic characterization

The transmittance and reflectance spectra of thin film samples of 4-methyl-TPD (solid curves) and TPD(4M)–MEH–P–PPV (dashed curves) on fused silica substrates are shown in Fig. 2. The absorption coefficient spectra and refractive index spectra derived from Fig. 2 are displayed in Fig. 3 (procedure is described in [47,48]). The Fresnel equation analysis [47,48] additionally gives the film thickness. The refractive index spectra of the films are considerably larger than the refractive index spectra of fused silica or of optical glass used as substrate. Therefore, waveguiding of radiation occurs in the films if they are thicker than a critical film thickness, ℓ_{crit} [51]. The required critical film thickness values for waveguiding in the films on BK7 glass at the wavelength of peak amplified spontaneous emission are listed in Table 2.

The absorption cross-section spectra, $\sigma_a(\lambda)$, of 4-methyl-TPD and TPD(4M)–MEH–P–PPV in dioxane (dashed curves) and as neat films (solid curves) are shown in Fig. 4. For the liquid solutions, $\sigma_a(\lambda)$ is determined from transmission measurements using the relation $T(\lambda) = \exp[-\sigma(\lambda)N_{RU}\ell]$, where N_{RU} is the number density of molecules or repeat units, and ℓ the sample length. The absorption cross-section spectra of the neat films are determined by assuming equal absorption cross-section integrals for the $S_0 - S_1$ absorption bands (upper wavelength borders λ_u). The relation $\sigma_{a,f}(\lambda) = \alpha_f(\lambda) \int \sigma_{a,s}(\tilde{\nu})\, d\tilde{\nu} / \int \alpha_f(\tilde{\nu})\, d\tilde{\nu}$ is used, where $\tilde{\nu} = \lambda^{-1}$ is the wavenumber, the subscripts 'f' and 's' stand for neat film and solution, respectively. The

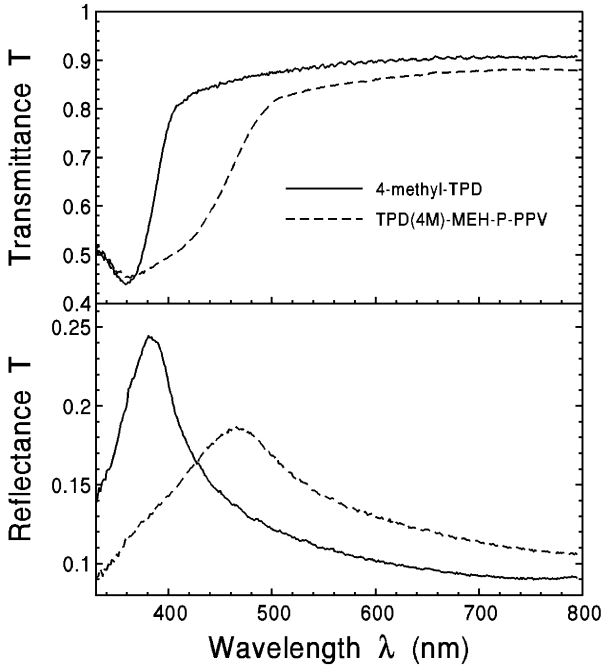

Fig. 2. Transmittance, $T(\lambda)$, and reflectance, $R(\lambda)$, spectra. Solid curves: 38 nm thick film of 4-methyl-TPD on fused silica. Dashed curves: 60 nm thick film of TPD(4M)–MEH–P–PPV on fused silica.

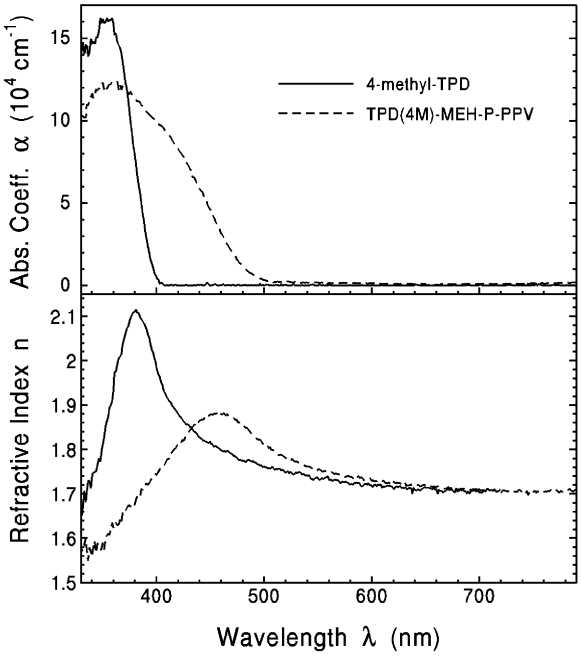

Fig. 3. Absorption coefficient spectra, $\alpha(\lambda)$, and refractive index spectra, $n(\lambda)$. Solid curves: 4-methyl-TPD. Dashed curves: TPD(4M)–MEH–P–PPV.

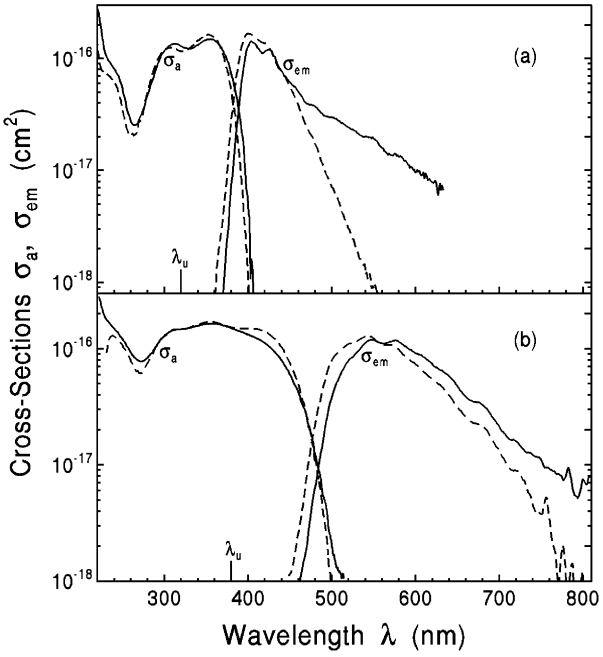

Fig. 4. Absorption cross-section spectra, $\sigma_a(\lambda)$, and stimulated emission cross-section spectra, $\sigma_{em}(\lambda)$, of neat films (solid curves) and 1,4-dioxane solutions (dashed curves). (a) 4-Methyl-TPD (molecular based). (b) TPD(4M)–MEH–P–PPV (repeat unit based).

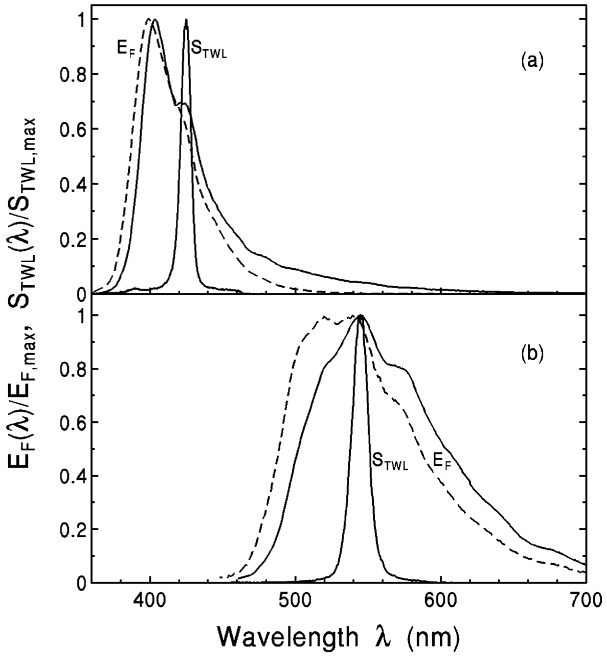

Fig. 5. Normalized fluorescence quantum distributions, $E_F(\lambda)/E_{F,max}$, and normalized traveling wave laser spectra, $S_{TWL}(\lambda)/S_{TWL,max}$. Solid curves: neat films. Dashed curves: 1,4-dioxane solutions. (a) 4-Methyl-TPD. (b) TPD(4M)–MEH–P–PPV.

number density, N_{RU}, of molecules or repeat units in neat films is obtained by the relation $N_{RU} = \alpha_f(\lambda)/\sigma_{a,f}(\lambda)$. Values of N_{RU} are listed in Table 2.

The absorption cross-section spectrum of 4-methyl-TPD exhibits two overlapping peaks at 360 and 310 nm. They are thought to belong to two electronic transitions, $S_0 \rightarrow S_1$ and $S_0 \rightarrow S_2$. The solution spectrum is approximately 6 nm blue shifted compared to the neat film spectrum. Otherwise, both the spectra have a similar shape.

The absorption cross-section spectrum of TPD(4M)–MEH–P–PPV exhibits three overlapping peaks at 420, 360 and 310 nm. They are thought to belong to three electronic transitions, $S_0 \rightarrow S_1$, $S_0 \rightarrow S_2$, and $S_0 \rightarrow S_3$. Below 380 nm, the absorption cross-section spectra of TPD(4M)–MEH–P–PPV and 4-methyl-TPD are quite similar. The bridging of 4-methyl-TPD with vinylene–MEH–phenylene–vinylene units adds only the long-wavelength band centered around 420 nm. There seems to be only a coupling of the TPD and the MEH-substituted vinylene–phenylene–vinylene chromophores, but not a complete merging to a single chromophore. The absorption spectra of TPD(4M)–MEH–P–PPV neat films and of TPD(4M)–MEH–P–PPV in dioxane solution are spectrally unshifted. Only the solution spectrum has a more strongly pronounced $S_0 - S_1$ absorption peak than the neat film.

Normalized fluorescence quantum distributions, $E_F(\lambda)/E_{F,max}$, for dioxane solutions and neat films of 4-methyl-TPD (part a) and TPD(4M)–MEH–P–PPV (part b) are shown in Fig. 5. The solution spectrum of 4-methyl-TPD is approximately 6 nm blue shifted compared to the neat film spectrum as is the absorption spectrum. The vibronic structure is more pronounced for the neat film than for the solution. The fluorescence spectrum of TPD(4M)–MEH–P–PPV in dioxane is slightly blue shifted and has a steeper short-wavelength rise than the fluorescence spectrum of the TPD(4M)–MEH–P–PPV neat films. The wavelengths of maximum fluorescence, $\lambda_{F,max}$, of 4-methyl-TPD and of TPD(4M)–MEH–P–PPV are listed in Table 1.

The determined fluorescence quantum yields are $\phi_F = \int_{em} E_F(\lambda)\,d\lambda = 0.26$ (0.6) for 4-methyl-TPD neat films (dioxane solutions), and 0.52 (0.53) for TPD(4M)–MEH–P–PPV neat films (dioxane solutions). In 4-methyl-TPD neat films, the fluorescence quantum yield is reduced by more than a factor of 2 compared to solution, while for TPD(4M)–MEH–P–PPV the fluorescence quantum yield is high and practically the same in solution and in neat film.

The temporal fluorescence signals of a neat film (thickness 3 nm, transmission $T_0 = 0.95$, solid curve) and of a dioxane solution (cell thickness 1 mm, $T_0 = 0.88$, dashed curve) of 4-methyl-TPD are shown in Fig. 6a. The deduced fluorescence lifetimes are $\tau_F(\text{solution}) = (1.1 \pm 0.1)$ ns and $\tau_F(\text{neat film}) = (0.29 \pm 0.05)$ ns. The temporal fluorescence signals of a neat film (thickness 6 nm, transmission $T_0 = 0.934$, solid curve) and of a dioxane solution (cell thickness 1 mm, $T_0 = 0.97$, dashed curve) of TPD(4M)–MEH–P–PPV are shown in Fig. 6b. The deduced fluorescence lifetimes are $\tau_F(\text{solution}) = (1.29 \pm 0.04)$ ns and $\tau_F(\text{neat film}) = (0.81 \pm 0.06)$ ns. The dotted curves in Fig. 6a and b give the system response functions (signals

Table 1
Spectroscopic parameters of 4-methyl-TPD, 3-methyl-TPD, poly-TPD(4M)–DPX, TPD(4M)–MEH–P–DPV, and TPD(4M)–MEH–PPV at room temperature

Parameter	4-Methyl-TPD		3-Methyl-TPD		Poly-TPD(4M)–DPX Neat film	TPD(4M)–MEH–P–PPV		TPD(4M)–MEH–PPV	
	Neat film	1,4-Dioxane	Neat film	1,4-Dioxane		Neat film	1,4-Dioxane	Neat film	1,4-Dioxane
ϕ_F	0.26	0.60	0.4	0.69	0.125	0.49 ± 0.02	0.53 ± 0.01	0.14	0.79
τ_F (ns)	0.29 ± 0.05	1.08 ± 0.08	0.44 ± 0.05	1.4 ± 0.1	0.254 ± 0.045	0.81 ± 0.06	1.29 ± 0.04	0.182 ± 0.05	1.23 ± 0.09
$\tau_{rad,lum}$ (ns)	1.1	1.8	1.1	2.0	2.0 ± 0.4	1.65	2.43	1.27	1.55
$\tau_{rad,RU}$ (ns)	1.4	2.1	1.0	1.92	1.83	3.06	4.0	1.68	1.86
m_{lum}	1.3		1		1	1.8	1.6	1.3	1.2
P_F	≈0.022	0.145	≈0.01	0.14		0.022	0.104	≈0.019	0.045
τ_{or} (ps)	≈11	≈370	≈8	≈400		≈31	≈280	≈6	≈100
$\lambda_{a,max}$ ($S_0 - S_1$) (nm)	357	354	357	353	353	≈410	410	429	438
$\lambda_{F,max}$ (nm)	403.5	399.5	399	393	410	545	542	538	495

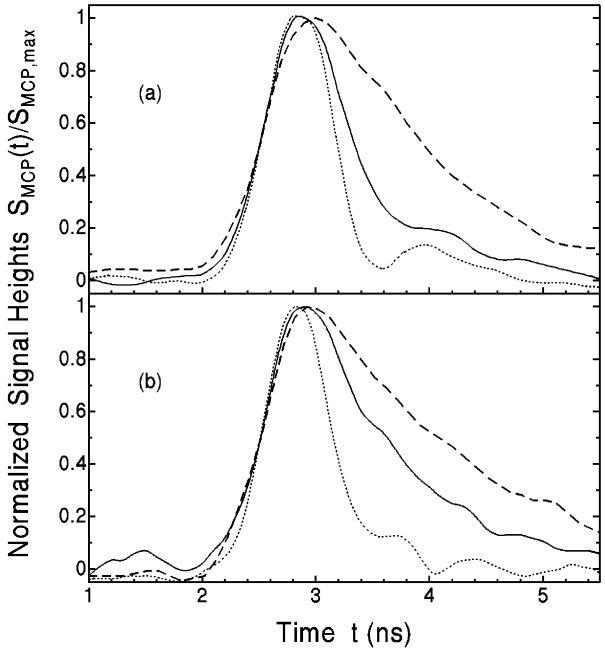

Fig. 6. Temporal fluorescence signal traces of neat films (solid curves) and 1,4-dioxane solutions. Normalized micro-channel-plate photomultiplier signal heights are presented. Dotted curves show instrumental response function. (a) 4-Methyl-TPD. (b) TPD(4M)–MEH–P–PPV.

detected by directly measuring an attenuated pump pulse of 35 ps duration).

The radiative lifetimes of the lumiphores (emitting chromophores), $\tau_{rad,lum}$, are determined by the measured fluorescence lifetimes, τ_F, and fluorescence quantum yields, ϕ_F, according to $\tau_{rad,lum} = \tau_F/\phi_F$. The obtained values are listed in Table 1. Additionally, the repeat unit-based radiative lifetimes, $\tau_{rad,RU}$, are calculated by using the Strickler–Berg formula [52,53] (see Eq. (2) in [36]) and listed in Table 1. The number of repeat units, m_{lum}, forming an emitting chromophore is given by $m_{lum} = \tau_{rad,RU}/\tau_{rad,lum}$. For TPD(4M)–MEH–P–PPV neat films the lumiphore is found to comprise approximately two repeat units. In dioxane solution, the average lumiphore size is approximately 1.6 repeat units (see Table 1). For 4-methyl-TPD neat films the average lumiphore size is approximately equal to the molecule size.

The degree of fluorescence polarization, $P_F = (S_{F,\parallel} - S_{F,\perp})/(S_{F,\parallel} + S_{F,\perp})$, of the samples was determined by measuring the fluorescence signal polarized parallel ($S_{F,\parallel}$) and perpendicular ($S_{F,\perp}$) to the polarization of the excitation light. The reorientation time, τ_{or}, of the $S_0 - S_1$ transition dipole moments is calculated form the degree of fluorescence polarization [54,55] (see Eq. (5) in [36]). For TPD(4M)–MEH–P–PPV neat films the degree of fluorescence polarization is low and the reorientation time is short because of intra-chain and inter-chain migration of the excitation energy. In liquid solution, the degree of fluorescence polarization and the reorientation time are larger than in neat films because only intra-chain energy migration occurs and the chains may not be completely curled up. In the case of 4-methyl-TPD in dioxane, the degree of fluorescence polarization is determined by the molecular reorientation within the fluorescence lifetime (reorientation of transition dipole moments is equal to the molecular reorientation time). 4-Methyl-TPD neat films have a low degree of fluorescence polarization and a short reorientation time of the transition dipole moments because of excited state energy migration to neighboring molecules of different orientation.

The repeat unit-based stimulated emission cross-section spectra, $\sigma_{em}(\lambda)$, presented in Fig. 4 are calculated from the fluorescence quantum distributions, $E_F(\lambda)$ (Fig. 5) and the $S_0 - S_1$ radiative lifetimes, $\tau_{rad,RU}$, by the application of relations between the Einstein A and B coefficients [56,57] (see Eq. (3) in [36]). The absolute values are not too accurate because of the uncertainties in the position of the upper limit, λ_u, of the $S_0 - S_1$ absorption bands.

3.2. Wave-guided traveling wave lasing

For the traveling wave laser studies neat films on microscope objective slides were prepared. The film thickness values are listed in Table 2. The pump pulse cross-sectional area at the samples was $A = 17\,\text{mm} \times 0.19\,\text{mm}$. The samples were covered to restrict the exposed length to $\ell = 5\,\text{mm}$. The solid angle of amplified spontaneous light acceptance is $\Delta\Omega = 0.16\,\text{sr}$.

In Fig. 5, the normalized wave-guided traveling wave laser (wave-guided amplified spontaneous emission) spectra, $S_{TWL}(\lambda)/S_{TWL,max}$, obtained well above threshold are included. The wavelength of peak emission, $\lambda_{TWL,max}$, coincides with the first vibronic shoulder for 4-methyl-TPD. In the case of TPD(4M)–MEH–P–PPV, it approximately coincides with the wavelength position of peak fluorescence emission which seems to be the first vibronic band.

The dependencies of the traveling wave laser output, W_{TWL}, the wavelength of peak emission, $\lambda_{TWL,max}$, and the spectral width of the emission, $\Delta\lambda_{TWL}$ (FWHM), on the input pump pulse energy density, w_{0L}, are shown in Fig. 7 for 4-methyl-TPD and in Fig. 8 for TPD(4M)–MEH–P–PPV. Above a certain threshold pump pulse energy density, $w_{L,th}$, the emission begins to rise beyond the spontaneous emission level due to stimulated emission. At high pump pulse energy densities, the output signal saturates to $W_{TWL,max}$. The saturation is thought to be due to exciton–exciton annihilation processes at high densities of excited repeat units [58,59]. The solid curves in Figs. 7a and 8a are calculated by using the relation [29,32]

$$W_{TWL} = W_{TWL,max}\left\{1 - \exp\left[-\frac{(w_{0L} - w_{L,th})}{(w_{L,g,sat} - w_{L,th})}\right]\right\} \quad (1)$$

where $w_{L,g,sat}$ is the pump pulse energy density of gain saturation. Values of $w_{L,th}$, $w_{L,g,sat}$, and $W_{TWL,max}$ are listed in Table 2. The initial laser slope efficiencies, $\eta_{sl,ini}$, at

Table 2
Physical parameters and laser characterization of 4-methyl-TPD, 3-methyl-TPD, poly-TPD(4M)–DPX, TPD(4M)–MEH–P–PPV, and TPD(4M)–MEH–PPV neat films at room temperature

Parameter	4-Methyl-TPD	3-Methyl-TPD	Poly-TPD(4M)-DPX	TPD(4M)–MEH–P–PPV	TPD(4M)–MEH–PPV
M_{RU}(g mol^{-1})	516.69	516.69	770.9	953.28	801.04
M_n (g mol^{-1})	516.69	516.69	11,300	9,200	14,600
M_w (g mol^{-1})	516.69	516.69	44,300	16,300	53,100
T_g (°C)	163	168	≈240	169	188
N_{RU} ($\times 10^{20}$ cm^{-3})	11.5	10.6	6.2	7.7	6.4
ℓ_{crit} (nm)	48.7	51.1	93	87.6	94
d_f (nm)	195	66	≈100	215	100
$d_{abs,L}$ (nm)	60	67	95	81	108
$\sigma_{a,L}$ ($\times 10^{-16}$ cm^2)	1.44	1.41	1.7	1.6	1.45
$\lambda_{TWL,max}$ (nm)	422	418	421	544	540
$\Delta\lambda_{TWL}$ (nm)	6.5	6.6	6.6	13	7.4
$w_{L,1/2}$ (μJ cm^{-2})	20	20	62	17	8
$w_{L,th}$ (μJ cm^{-2})	20	20	60	11	8
$w_{L,g,sat}$ (μJ cm^{-2})	1200	900	550	600	218
$W_{TWL,max}$ (nJ)	9	55	24	31	17
ℓ_{TWL} (mm)	≈0.45	≈0.9	≈1	≈1.4	≈1
$\sigma_{em}(\lambda_{TWL,max})$ ($\times 10^{-16}$ cm^2)	1.18	1.59	≈1.6	1.31	2.35
$\sigma_{em,eff}(\lambda_{TWL,max})$ ($\times 10^{-17}$ cm^2)	6.75	3.1	≈3.2	3.3	≈11
$\eta_{sl,ini}$	0.0008	0.003	0.0052	0.0055	0.0085

threshold concerning the collected TWL light are obtained from Eq. (1) by

$$\eta_{sl,ini} = \frac{1}{A_{exc}} \frac{\partial W_{TWL}}{\partial w_{0L}}\bigg|_{w_{0L}=w_{L,th}} = \frac{1}{A_{exc}} \frac{W_{TWL,max}}{w_{L,g,sat} - w_{L,th}} \quad (2)$$

where A_{exc} is the exposed film area. The calculated values $\eta_{sl,ini}$ are listed in Table 2. It should noted that the true initial laser slope efficiency is larger since the traveling wave laser emission occurs in forward and backward direction along the pump line focus and the emission angle at the film edge

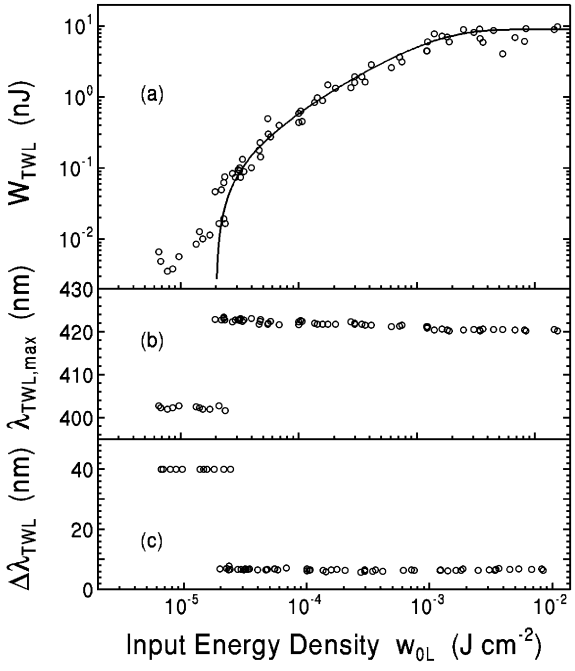

Fig. 7. Wave-guided traveling wave laser performance of 4-methyl-TPD. (a) Collected emission signal, W_{TWL}, vs. input pump pulse peak energy density, w_{0L}. Pumped film area: 0.19 mm × 5 mm. Curve is calculated by use of Eq. (1) with $w_{L,th} = 20$ μJ cm^{-2}, $w_{L,g,sat,} = 1.2$ mJ cm^{-2}, and $W_{TWL,max} = 9$ nJ. (b) Peak wavelength of traveling wave laser, $\lambda_{TWL,max}$, vs. input pump pulse peak energy density, w_{0L}. (c) Spectral linewidth (FWHM) of traveling wave laser, $\Delta\lambda_{TWL}$, vs. input pump pulse peak energy density, w_{0L}.

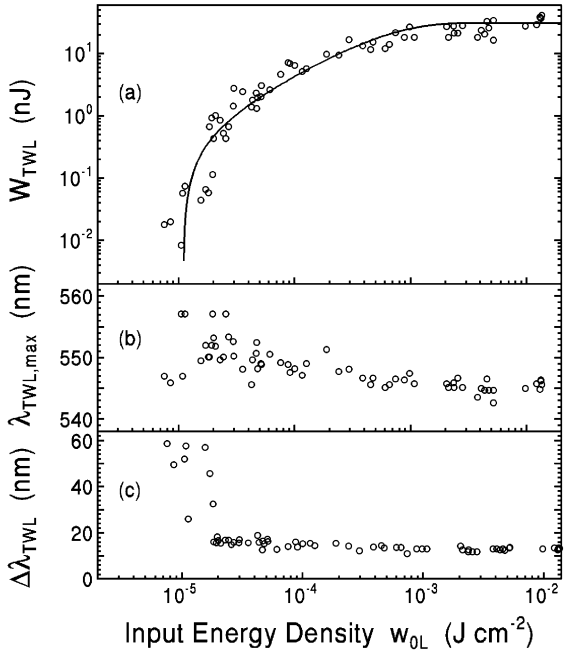

Fig. 8. Wave-guided traveling wave laser performance of TPD(4M)–MEH–P–PPV. (a) Collected emission signal, W_{TWL}, vs. input pump pulse peak energy density. Pumped film area: 0.19 mm × 5 mm. Curve is calculated by use of Eq. (1) with $w_{L,th} = 11$ μJ cm^{-2}, $w_{L,g,sat} = 0.6$ mJ cm^{-2}, and $W_{TWL,max} = 31$ nJ. (b) Peak wavelength of traveling wave laser, $\lambda_{TWL,max}$, vs. input pump pulse peak energy density, w_{0L}. (c) Spectral linewidth (FWHM) of traveling wave laser, $\Delta\lambda_{TWL}$, vs. input pump pulse peak energy density, w_{0L}.

is larger than the acceptance angle of the collecting lens ($\Delta\theta = 0.6$ rad).

The wavelength of peak ASE emission, $\lambda_{TWL,max}$, shifts from 423 nm at laser threshold to 421 nm at high excitation energy density for 4-methyl-TPD, while for TPD(4M)–MEH–P–PPV it shifts from 553 nm at laser threshold to about 544 nm at high excitation energy density (Figs. 7b and 8b). The sharp first vibronic fluorescence peak of 4-methyl-TPD pins the ASE emission wavelength to a fixed position with small shot-to-shot fluctuation and small excitation energy dependence (Fig. 7b). In the case of TPD(4M)–MEH–P–PPV the first vibronic fluorescence band is broad and therefore the peak ASE wavelength position fluctuates somewhat from shot to shot and varies somewhat with the excitation energy density (Fig. 8b).

Around the laser threshold, the spectral width of emission, $\Delta\lambda_{TWL}$, reduces rapidly from the fluorescence spectral width to the TWL spectral width. The dependence of $\Delta\lambda_{TWL}$ on the pump pulse energy density is displayed in Figs. 7c and 8c. The spectral width of the ASE emission of 4-methyl-TPD ($\Delta\lambda_{TWL} \approx 6.5$ nm) is narrower than that of TPD(4M)–MEH–P–PPV ($\Delta\lambda_{TWL} \approx 13$ nm) because of the smaller first vibronic fluorescence bandwidth of 4-methyl-TPD. A discussion of the traveling wave laser or amplified spontaneous emission spectral narrowing as a function of the excitation energy density is found in [24,60,61]

The effective gain lengths, ℓ_{TWL}, of light amplification have been determined by measuring the threshold pump pulse energy density, $w_{L,th}$, as a function of the transverse pumping length, ℓ_{ap}, as described in [24] (threshold energy density, $w_{L,th}$, increases when $\ell_{ap} < \ell_{TWL}$). The determined gain lengths are listed in Table 2.

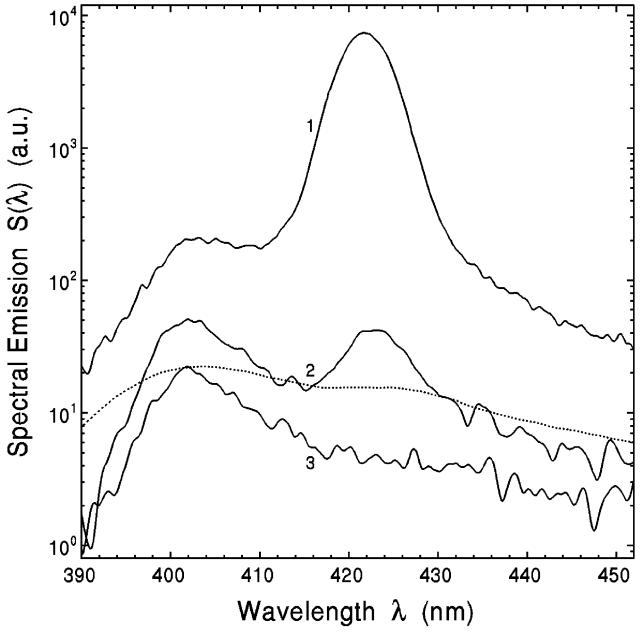

Fig. 9. Edge emission of fluorescence and build-up of amplified spontaneous emission for a 4-methyl-TPD neat film on a glass substrate. Exposed film area by picosecond pump laser is 0.19 mm × 5 mm. Film thickness: $d_f = 200$ nm. The applied pump pulse energy densities are: (1) $w_{0L} = 6.9$ μJ cm^{-2}, (2) 23 μJ cm^{-2}, and (3) 160 μJ cm^{-2}. Dotted curve: shape of intrinsic fluorescence quantum distribution (solid curve in Fig. 5a) determined from front-face fluorescence collection.

The pump pulse energy density, $w_{L,1/2}$, required for spectral narrowing of the emission to half of its initial value is related to the effective stimulated emission cross-section, $\sigma_{em,eff}$, at $\lambda_{TWL,max}$ and the effective interaction length, ℓ_{TWL}. The lower $w_{L,1/2}$ and the shorter ℓ_{TWL}, the higher is $\sigma_{em,eff}$. The $\sigma_{em,eff}$ values listed in Table 2 have been determined by following the procedure described in [24]. The $\sigma_{em,eff}(\lambda)$ is always smaller than $\sigma_{em}(\lambda)$ because photo-induced absorption reduces the efficiency of light amplification.

The spectral development of the edge emission of the transverse excited 4-methyl-TPD neat film sample is shown in Fig. 9. The solid curve 3 was obtained using an excitation energy density of $w_{0L} = 6.8$ μJ cm^{-2} well below the threshold amplification of spontaneous emission. For comparison, the dotted curve shows the spectral distribution of the spontaneous emission in the front-face collection arrangement used for the fluorescence measurements (see solid $E_F(\lambda)$ curve in Fig. 5a). The wave-guided fluorescence in the thin film is spectrally modified. The solid curve 2 in Fig. 9 shows edge emission slightly above the threshold ($w_{0L} = 23$ mJ cm^{-2}) of observable amplification of spontaneous emission. A peak builds up around 424 nm. Curve 1 shows the situation at a pump pulse energy density of $w_{0L} = 160$ μJ cm^{-2}, approximately a factor of 8 above threshold. The wave-guided amplified spontaneous emission peaking at $\lambda_{TWL,max} = 422$ nm clearly dominates. Below the laser threshold, the fluorescence at propagation angles slightly below the angle of total internal reflection is preferentially emitted into the substrate in a small angle range to the film/substrate interface (leaky mode emission) at wavelengths fulfilling a constructive interference condition which is film thickness and refractive index dependent [62].

4. Discussion

The optical, spectroscopic, and lasing behaviour of 3-methyl-TPD neat films and solutions in dioxane were studied in [63]. The spectroscopic parameters of 3-methyl-TPD are included in Table 1. Both 4-methyl-TPD and 3-methyl-TPD behave roughly similar. The fluorescence spectrum of 3-methyl-TPD is a few nanometer blue shifted, and the fluorescence quantum yield of 3-methyl-TPD is slightly higher in solution as well as in neat film.

The lasing behaviour of 4-methyl-TPD and 3-methyl-TPD neat films is compared in Table 2. Both molecular films show laser action (laser wavelength around 420 nm). This is quite unusual for organic molecular films. Generally, organic laser dyes show no laser action as neat films because of enormous fluorescence quenching [33–35]. Only recently, amplified spontaneous emission was reported for several

spiro-type light-emitting molecules [37,38]. 3-Methyl-TPD exhibits a somewhat better laser performance (lower laser threshold $w_{L,th}$, longer effective amplification length ℓ_{TWL}, higher maximum output energy) than 4-methyl-TPD. This is probably due to the higher fluorescence quantum yield and the better film forming properties of 3-methyl-TPD.

The copolymerization of 4-methyl-TPD with α,α′-diphenylxylylene leads to a non-conjugated luminescent polymer, named poly-TPD(4M)–DPX, with similar absorption, fluorescence, and lasing properties as 4-methyl-TPD. The results are published in [32]. The structural formula of poly-TPD(4M)–DPX is included in Fig. 1, the neat film spectroscopic properties are included in Table 1, and the neat film lasing properties of poly-TPD(4M)–DPX are included in Table 2. Also, the copolymerization of 3-methyl-TPD with α,α′-diphenylxylylene leads to a non-conjugated luminescent polymer, named poly-TPD–DPX, with similar spectroscopic and lasing behaviour [30]. Since there is no conjugated bridge between the TPD units, the absorption, fluorescence and wave-guided traveling wave laser spectra are nearly unchanged by the polymerization process.

On the other hand, the bridging of 4-methyl-TPD with phenylvinylene–MEH–phenylene–phenylvinylene units (TPD(4M)–MEH–P–PPV) or with vinylene–MEH–phenylene–vinylene units (TPD(4M)–MEH–PPV) leads to conjugated luminescent polymers which emit in the green to red spectral region and show amplified spontaneous emission around 540 nm. The optical, spectroscopic and lasing behaviour of TPD(4M)–MEH–PPV has been investigated already previously [32]. Results are included in Tables 1 and 2.

The short-wavelength behaviour ($\lambda < 400$ nm) of TPD(4M)–MEH–P–PPV (Fig. 4 of this paper) and of TPD(4M)–MEH–PPV (Fig. 5 of [32]) is quite similar to the absorption behaviour of 4-methyl-TPD and 3-methyl-TPD. There seems to be only a coupling of the vinylene–MEH–phenylene–vinylene chromophores with the TPD chromophores due to the conjugation but not a complete merging into a new single chromophore with a new level structure. The $S_0 - S_1$ absorption band of TPD(4M)–MEH–PPV is a factor of two stronger than the $S_0 - S_1$ absorption band of TPD(4M)–MEH–P–PPV. The additional phenyl groups lower the absorption strength. TPD(4M)–MEH–PPV in dioxane has a higher fluorescence quantum yield than TPD(4M)–MEH–P–PPV in the same solvent, but in solid state the fluorescence quantum yield of TPD(4M)–MEH–PPV is reduced to 14% while the fluorescence quantum yield of TPD(4M)–MEH–P–PPV remains unchanged (≈53%). The average lumiphore size (coherent exciton extension) of TPD(4M)–MEH–P–PPV extends over about two repeat units while for TPD(4M)–MEH–PPV it is restricted to nearly one repeat unit. The phenyl groups seem to increase the near-field order.

Comparing the laser performance, the laser threshold for TPD(4M)–MEH–P–PPV is somewhat higher than for TPD(4M)–MEH–PPV probably due to the lower stimulated emission cross-section at similar photo-induced absorption. Both polymers emit at approximately the same laser wavelength. The effective amplification length is similar. Gain saturation occurs at higher pump pulse energy densities and the maximum TWL output is higher for TPD(4M)–MEH–P–PPV, probably due to weaker exciton–exciton annihilation.

In comparison to MEH–PPV [12,24], TPD(4M)–MEH–P–PPV as well as TPD(4M)–MEH–PPV perform reasonably well. The relevant MEH–PPV parameters are $\lambda_{TWL,max} = 627$ nm, $w_{L,th} = 8\ \mu J\ cm^{-2}$, $\ell_{TWL} \approx 1$ mm, $w_{L,g,sat} = 690\ \mu J\ cm^{-2}$, and $W_{TWL,max} = 2.8$ nJ. The TPD(4M)–MEH–P–PPV and TPD(4M)–MEH–PPV copolymers emit at shorter wavelength and therefore have their own importance.

5. Conclusions

4-Methyl-TPD, a low molar mass luminescent molecule, and TPD(4M)–MEH–P–PPV, a high molar mass luminescent conjugated polymer, have been characterized by optical spectroscopy in liquid solution (dioxane) and as neat films. Traveling wave lasing was achieved for both neat film samples with good performance data. Both compounds combine good electro-luminescence properties [29,64,65] with optical laser properties which make them candidates for electro-injection lasers [5,66].

A comparison of 4-methyl-TPD with 3-methyl-TPD has been undertaken to show that there is no significant influence of the optical, spectroscopic and lasing properties on the methyl position. The laser action is around 420 nm. However, 3-methyl-TPD has the advantage of better film forming properties. The conjugated copolymers TPD(4M)–MEH–P–PPV and TPD(4M)–MEH–PPV have been compared to illustrate the influence of the substitution of an H atom by a phenyl group at the vinylene position. Both polymers show reasonably good laser action in neat films around 540 nm. TPD(4M)–MEH–P–PPV has a slightly higher laser threshold but gives a somewhat higher laser output at high excitation intensity. A comparison of 4-methyl-TPD with non-conjugated poly-TPD(4M)–DPX shows that copolymerization resulting in a non-conjugating bridge has little influence on the spectroscopic and lasing properties. In contrast, the comparison of 4-methyl-TPD molecules with conjugated TPD(4M)–MEH–P–PPV has clarified the influence of the other type of copolymerization which results in a conjugating bridge consisting of vinylene–MEH–phenylene–vinylene units between the 4-methyl-TPD units. This special type of copolymerization leads to a coupling of the TPD and vinylene–MEH–phenylene–vinylene chromophores which retains the absorption structure of TPD but only adds a long-wavelength absorption band from the polyconjugation. The latter is responsible for the shift of the laser spectrum to 540 nm.

The lasing studies have been restricted to wave-guided traveling wave lasing (wave-guided amplification of spontaneous emission) in this paper. But whenever traveling

wave lasing (laser generator operation) is possible then laser oscillator operation (like distributed-feedback laser action [3,13,26], micro-cavity laser action [27,67], or micro-ring laser action [4,68,69]) may be achieved in appropriate resonator structures since feedback lowers the laser threshold.

Acknowledgements

We thank the Commission of the European Communities for support under the ESPRIT contract 28580 "A Novel Approach to Solid State Wavelength Laser Generation Using Luminescent Polymers (LUPO)" which enabled this collaborative work.

Appendix A. Synthesis details for TPD(4M)–MEH–PPV and TPD(4M)–MEH–P–PPV

The synthesis pathway starting from 4-methyl-TPD is outlined in the synthetic scheme of Fig. 10 and includes the preparation of both monomers, the TPD-dialdehyde and TPD-diketone by Vilsmeier formylation and Friedl–Crafts acylation, respectively. Solution processable high molecular polymers were prepared through the well-established polycondensation route employing the repetitive Horner-type carbonylolefination of dialdehydes and diketons with xylylene bis(phosphonates) [12,29,31]. The obtained polymer structures are well-defined and in full agreement with the molecular formulae (see below) as shown by number and position of the signals in the ^{13}C NMR and ^{1}H NMR spectra. Molecular weight distribution is analyzed by gel permeation chromatography (GPC) showing M_w/M_n polydispersity index between 1.8 and 3.6. The polymers are completely soluble in THF, dioxane, toluene, chlorobenzene, and by solution casting amorphous transparent films were formed. The glass transition temperatures reached high values in the range of 160–190 °C which is important for the thermal stability of the device structures constructed with these materials.

A.1. Synthesis of TPD(4M)–MEH–PPV: poly[(4-methylphenyl)imino-4,4′-diphenylene-(4-methylphenyl)imino-1,4-phenylene-ethenylene-2-methoxy-5-(2-ethylhexyloxy)-1,4-phenylene-ethenylene-1,4-phenylene]

2-Methoxy-5-(2-ethylhexyloxy)-1,4-xylylene-bis(diethylphosphonate) (5.365 g; 10 mmol) and *N*,*N*′-bis(4-formylphe-

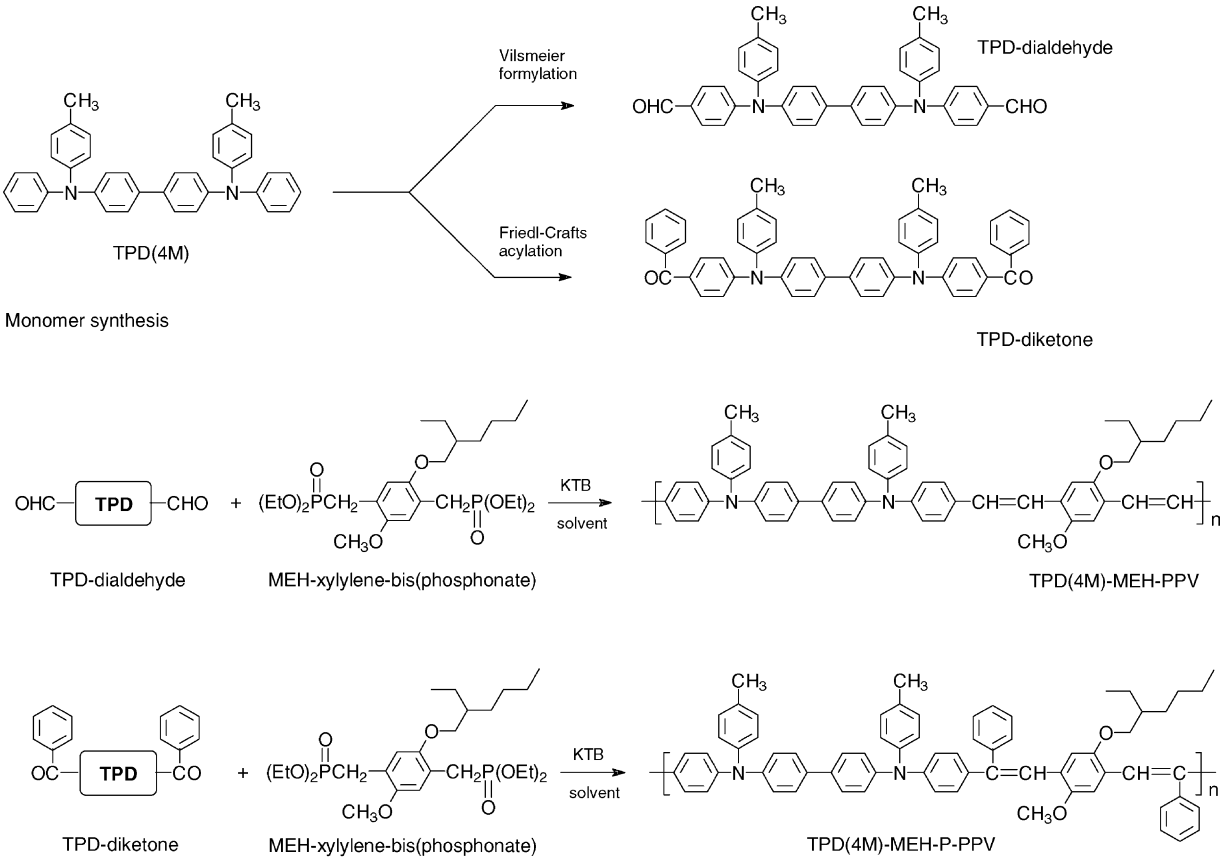

Fig. 10. Synthetic scheme for the preparation of the investigated TPD–PPVs via the polycondensation route employing the repetitive Horner-type carbonyl olefination.

nyl)-*N*,*N*′-bis(4-methylphenyl)benzidine (5.726 g; 10 mmol) were dissolved in dry toluene (100 ml) whilst being stirred under argon and heating to reflux. To this solution solid potassium-*tert*-butoxide (3.36 g; 30 mmol) was added in one portion. After 4 h at reflux, the reaction mixture was quenched with aqueous HCl (100 ml) and diluted with additional toluene. The organic layer was then separated, washed several times with distilled water and dried in a Dean–Stark apparatus. The viscous polymer solution was diluted with additional toluene, centrifuged, then reduced by rotary evaporation, and precipitated into acetone. The crude polymer was extracted with methanol for 10 h and reprecipitated from toluene/methanol to give brilliant yellow fibers with a yield of 5.8 g (72%). For T_g and molecular weight, see Table 2.

FTIR (ATR) ν (cm^{-1}): ν(CH) 3024 (Ph); ν_{as}(CH), ν_s(CH) 2925, 2861 (aliphatic CH); ν(C–C) 1598, 1506, 1491 (Ph-breathing); ν(C–N) 1270 (N–Ph); ν(C–O) 1205, 1036 (Ph–O–C); γ(CH) 962 (*trans*-vinylene). ^{13}C NMR (400 MHz; CD_2Cl_2) δ (ppm): 151.7, 151.5, 147.6, 147.0, 145.1, 134.9, 133.8, 132.3, 132.2, 130.7, 130.4, 128.5, 128.3, 127.6, 127.57, 127.5, 127.0, 126.8, 125.7, 124.3, 123.5, 123.4, 121.8, 121.6, 110.2, 109.1, 72.1, 56.6, 40.2, 31.3, 29.6, 24.6, 23.5, 20.9, 14.3, 11.4. ^{1}H NMR (400 MHz; CD_2Cl_2) δ (ppm): 7.5–7.0 (m, 30H), 3.96–3.9 (d + s, 5H), 2.3 (s, 6H), 1.9–1.3 (m, 9H), 0.98 + 0.9 (2t, 6H). Anal.·Calc. for $(C_{57}H_{56}N_2O_2)_n$ $(801.04)_n$: C, 85.46; H, 7.05; N, 3.50. Found: C, 84.00; H, 7.59; N, 3.43.

A.2. Synthesis of TPD(4M)–MEH–P–PPV: poly[(4-methylphenyl)imino-4,4′-diphenylene-(4-methylphenyl)imino-1,4-phenylene-1-phenyl-ethenylene-2-methoxy-5-(2-ethylhexyloxy)-1,4-phenylene-2-phenyl-ethenylene-1,4-phenylene]

2-Methoxy-5-(2-ethylhexyloxy)-1,4-xylylene-bis(diethylphosphonate) (5.365 g; 10 mmol) and *N*,*N*′-bis(4-benzoylphenyl)-*N*,*N*′-bis(4-methylphenyl)benzidine (7.249 g; 10 mmol) were dissolved in dry chlorobenzene (40 ml) whilst being stirred under argon and heating to reflux. To this solution solid potassium-*tert*-butoxide (3.36 g; 30 mmol) was added in one portion. After 4 h at reflux, the resulting viscous mixture was quenched with aqueous HCl (100 ml) and diluted with chlorobenzene (200 ml). The organic layer was then separated, washed several times with distilled water and dried in a Dean–Stark apparatus. The viscous polymer solution was centrifugated, then reduced by rotary evaporation, and precipitated into acetone (1 l). The crude polymer was extracted with methanol for 10 h and reprecipitated from toluene/methanol to give brilliant yellow fibers with a yield of 6.9 g (73%). For T_g and molecular weight, see Table 2.

FTIR (ATR) ν (cm^{-1}) ν(CH) 3027 (Ph); ν_{as}(CH), ν_s(CH) 2956, 2872 (aliphatic CH); ν(C–C) 1598, 1504, 1491 (Ph-breathing); ν(C–N) 1269 (N–Ph); ν(C–O) 1204, 1035 (Ph–O–C). Anal.·Calc. for $(C_{69}H_{64}N_2O_2)_n$ $(953.28)_n$: N, 2.94. Found: N, 2.90.

A.3. Synthesis of monomers: N,N′-bis(4-formylphenyl)-N,N'-bis(4-methylphenyl)-benzidine (TPD-dialdehyde)

At 0 °C, *N*,*N*-dimethylformamide (4.4 g; 60 mmol) was added dropwise to phosphorus oxychloride $POCl_3$ (9.2 g; 60 mmol) under stirring and exclusion of moisture. After 20 min, a solution of *N*,*N*′-bis(4-methylphenyl)-*N*,*N*′-diphenyl benzidine (10.3 g; 20 mmol) in 1,2-dichloroethane (60 ml) was added dropwise to the solid DMF/$POCl_3$ complex, and the reaction mixture was stirred for 24 h at 70 °C. Then, the mixture was hydrolyzed in ice water and the residue was extracted with chloroform. The organic layer was washed several times with distilled water, dried over Na_2SO_4 and the solvent completely removed. After dissolving in toluene, the dark green crude product was chromatographed over silica gel/toluene and precipitated into petroleum ether yielding 10 g (87%) of yellow crystals. T_m = 188−192 °C.

FTIR (ATR) ν (cm^{-1}): ν(C=O) 1682. ^{13}C NMR (CD_2Cl_2) δ (ppm): 190.4, 153.6, 145.9, 143.8, 136.9, 135.9, 131.4, 130.8, 129.5, 128.2, 127.1, 126.4, 119.4, 21.1. ^{1}H NMR (CD_2Cl_2) δ (ppm): 9.79 (s, 2 H, –CHO), 7.7–7.0 (m, 24 H, Ar), 2.37 (s, 6 H, $-CH_3$).Anal.·Calc. for $C_{40}H_{32}N_2O_2$ (572.67): C, 83.89; H, 5.63; N, 4.89. Found: C, 83.40; H, 5.79; N, 4.87.

A.4. N,N'-bis(4-benzoylphenyl)-N,N′-bis(4-methylphenyl)benzidine (TPD-diketone)

At 0 °C, benzoyl chloride (6.0 g; 42 mmol) was added dropwise to a suspension of fine-powdered aluminum trichloride (6.4 g; 48 mmol) in 1,2-dichloroethane (40 ml) under stirring and exclusion of moisture. After 20 min, a solution of *N*,*N*′-bis(4-methylphenyl)-*N*,*N*′-diphenyl benzidine (10.33 g; 20 mmol) in 1,2-dichloroethane (40 ml) was added dropwise at 0–5 °C and then stirred for 3 days at 70 °C. Then the mixture was hydrolyzed in ice water/HCl and extracted with 1,2-dichloroethane. The organic layer was washed several times with distilled water and dried over Na_2SO_4. After the removal of the solvent, the dark green crude product was dissolved in toluene, chromatographed over silica gel/toluene and precipitated into petroleum ether yielding 9.7 g (78%) of a yellow powder. T_m = 238–244 °C.

FTIR (ATR) ν (cm^{-1}): ν(C=O) 1642. ^{13}C NMR (CD_2Cl_2) δ (ppm): 195.0, 152.2, 146.1, 144.1, 138.9, 136.5, 135.5, 132.2, 131.9, 130.7, 129.9, 129.7, 128.5, 128.0, 126.8, 126.0, 119.5, 21.1. ^{1}H NMR (CD_2Cl_2) δ (ppm): 7.8–7.5 (m, 18 H, Ar), 7.2–7.0 (m, 16 H, Ar), 2.36 (s, 6 H, $-CH_3$). Anal.·Calc. for $C_{52}H_{40}N_2O_2$ (724.86): C, 86.16; H, 5.56; N, 3.86. Found: C, 85.77; H, 5.95; N, 3.81.

References

[1] F. Hide, M.A. Díaz-García, B.J. Schwartz, A.J. Heeger, Acc. Chem. Res. 30 (1997) 430.

[2] A. Penzkofer, W. Holzer, S.-H. Gong, D.D.C. Bradley, X. Long, A. Bleyer, W.J. Blau, A.P. Davey, in: V.J. Corcoran, T.A. Goldman (Eds.), Proceedings of the International Conference on LASERS'98, STS Press, McLean, VA, 1999, p. 394.
[3] U. Lemmer, A. Haugeneder, C. Kallinger, J. Feldmann, in: G. Hadziioannou, P. van Hutten (Eds.), Semiconducting Polymers: Chemistry, Physics and Engineering, Wiley-VCH, Weinheim, 1999, p. 309.
[4] S.V. Frolov, M. Shkunov, A. Fujii, K. Yoshino, Z.V. Vardeny, IEEE J. Quant. Electron. 36 (2000) 2.
[5] M.D. McGehee, A.J. Heeger, Adv. Mater. 12 (2000) 1655.
[6] U. Scherf, S. Riechel, U. Lemmer, R.F. Mahrt, Curr. Opin. Solid State Mater. Sci. 5 (2001) 143.
[7] G. Kranzelbinder, G. Leising, Rep. Prog. Phys. 63 (2000) 729.
[8] N. Tessler, Adv. Mater. 11 (1999) 363.
[9] D. Moses, Appl. Phys. Lett. 60 (1992) 3215.
[10] F. Hide, B.J. Schwartz, M.A. Díaz-García, A.J. Heeger, Synth. Met. 91 (1997) 35.
[11] W. Holzer, A. Penzkofer, S.-H. Gong, A. Bleyer, D.D.C. Bradley, Adv. Mater. 8 (1996) 974.
[12] H.-H. Hörhold, H. Tillmann, C. Bader, R. Stockmann, J. Nowotny, E. Klemm, W. Holzer, A. Penzkofer, Synth. Met. 119 (2001) 199.
[13] G. Kranzelbinder, E. Toussaere, J. Zyss, A. Pogantsch, E.W.J. List, H. Tillmann, H.-H. Hörhold, Appl. Phys. Lett. 80 (2002) 716.
[14] N. Tessler, G.J. Denton, R.H. Friend, Nature 382 (1996) 695.
[15] M.D. McGehee, R. Gupta, S. Veenstra, E.K. Miller, M.A. Díaz-García, A.J. Heeger, Phys. Rev. B 58 (1998) 7035.
[16] A.K. Sheridan, G.A. Turnbull, A.N. Safonov, I.D.W. Samuel, Phys. Rev. B 62 (2000) R11 929.
[17] W. Holzer, A. Penzkofer, S.-H. Gong, A.P. Davey, W.J. Blau, Opt. Quant. Electron. 29 (1997) 713.
[18] C. Zenz, W. Graupner, S. Tasch, G. Leising, K. Müllen, U. Scherf, Appl. Phys. Lett. 71 (1997) 2566.
[19] X. Long, M. Grell, A. Malinowski, D.D.C. Bradley, M. Inbasekaran, E.P. Woo, Opt. Mater. 9 (1998) 70.
[20] G. Heliotis, D.D.C. Bradley, G.A. Turnbull, I.D.W. Samuel, Appl. Phys. Lett. 81 (2002) 415.
[21] S.V. Frolov, M. Shkunov, Z.V. Vardeny, K. Tada, R. Hidayat, M. Hirohata, M. Taraguchi, T. Masuda, K. Yoshino, Jpn. J. Appl. Phys. 36 (1997) L1268.
[22] G.H. Gelinck, J.M. Warman, M. Remmers, D. Neher, Chem. Phys. Lett. 265 (1997) 320.
[23] H. Brouwer, V.V. Krasnikov, A. Hilberer, G. Hadziioannou, Adv. Mater. 8 (1996) 935.
[24] W. Holzer, A. Penzkofer, T. Schmitt, A. Hartmann, C. Bader, H. Tillmann, D. Raabe, R. Stockmann, H.-H. Hörhold, Opt. Quant. Electron. 33 (2001) 121.
[25] A. Penzkofer, W. Holzer, T. Schmitt, A. Hartmann, C. Bader, H. Tillmann, D. Raabe, H.-H. Hörhold, Proc. SPIE 4087 (2001) 635.
[26] W. Holzer, A. Penzkofer, T. Pertsch, N. Danz, A. Bräuer, H. Tillmann, C. Bader, H.-H. Hörhold, Appl. Phys. B 74 (2002) 333.
[27] T. Granlund, M. Theander, M. Berggren, M. Andersson, A. Ruseckas, V. Sundström, G. Björk, M. Granström, O. Inganäs, Chem. Phys. Lett. 288 (1998) 879.
[28] A. Penzkofer, W. Holzer, H.-H. Hörhold, H. Tillmann, D. Raabe, M. Helbig, in: V.J. Corcoran, T.A. Corcoran (Eds.), Proceedings of the International Conference on Lasers 2000, STS Press, McLean, VA, 2001, p. 523.
[29] W. Holzer, A. Penzkofer, H. Tillmann, E. Klemm, H.-H. Hörhold, Synth. Met. 124 (2001) 455.
[30] W. Holzer, A. Penzkofer, H.-H. Hörhold, D. Raabe, M. Helbig, Opt. Mater. 15 (2000) 225.
[31] H.-H. Hörhold, H. Tillmann, D. Raabe, M. Helbig, W. Elflein, A. Bräuer, W. Holzer, A. Penzkofer, Proc. SPIE 4105 (2001) 431.
[32] W. Holzer, A. Penzkofer, H. Tillmann, D. Raabe, H.-H. Hörhold, Opt. Mater. 19 (2002) 283.
[33] F.P. Schäfer (Ed.), Dye Lasers, Topics in Applied Physics, vol. 1, 2nd revised ed., Springer-Verlag, Berlin, 1997.
[34] F.J. Duarte, L.W. Hillman (Eds.), Dye Laser Principles with Applications, Academic Press, Boston, 1990.
[35] A. Penzkofer, Y. Lu, Chem. Phys. 103 (1986) 399.
[36] W. Holzer, A. Penzkofer, H.-H. Hörhold, Synth. Met. 113 (2000) 281.
[37] N. Johansson, J. Salbeck, J. Bauer, F. Weisörtel, P. Broms, A. Anderson, W.R. Salaneck, Adv. Mater. 10 (1998) 1136.
[38] N. Johansson, J. Salbeck, J. Bauer, F. Weisörtel, P. Broms, A. Anderson, W.R. Salaneck, Synth. Met. 101 (1999) 405.
[39] T. Elsaesser, H.J. Polland, A. Seilmeier, W. Kaiser, IEEE J. Quant. Electron. 20 (1984) 191.
[40] S. Szatmari, F.P. Schäfer, Opt. Commun. 49 (1984) 281.
[41] J. Hebling, J. Kuhl, Opt. Lett. 14 (1978) 287.
[42] A. Penzkofer, W. Falkenstein, Opt. Quant. Electron. 10 (1978) 399.
[43] W. Falkenstein, A. Penzkofer, W. Kaiser, Opt. Commun. 27 (1978) 151.
[44] W.T. Sifvast, Laser Fundamentals, Cambridge University Press, Cambridge, 1996, p. 221.
[45] S.V. Frolov, M. Ozaki, W. Gellermann, Z.V. Vardeny, K. Yoshino, Jpn. J. Appl. Phys. 35 (1996) L1371.
[46] A. Penzkofer, Prog. Quant. Electron. 12 (1988) 291.
[47] A. Penzkofer, E. Drotleff, W. Holzer, Opt. Commun. 158 (1998) 221.
[48] W. Holzer, M. Pichlmaier, A. Penzkofer, D.D.C. Bradley, W.J. Blau, Opt. Commun. 163 (1999) 24.
[49] W. Holzer, M. Pichlmaier, A. Penzkofer, D.D.C. Bradley, W.J. Blau, Chem. Phys. 246 (1999) 445.
[50] W.H. Melhuish, J. Phys. Chem. 72 (1968) 2680.
[51] H. Kogelnik, in: T. Tamir (Ed.), Integrated Optics, Topics in Applied Physics, vol. 7, Springer-Verlag, Berlin, 1979, p. 13.
[52] S.J. Strickler, R.A. Berg, J. Chem. Phys. 37 (1962) 814.
[53] J.B. Birks, J. Dyson, Proc. R. Soc. London, Ser. A 275 (1963) 135.
[54] G. Weber, in: D.M. Hercules (Ed.), Fluorescence and Phosphorescence Analysis, Principles and Applications, Interscience, New York, 1966, p. 217.
[55] J.R. Lakowicz, Principles of Fluorescence Spectroscopy, Plenum Press, New York, 1983.
[56] O.G. Peterson, J.P. Webb, W.C. McColgin, J.H. Eberly, J. Appl. Phys. 42 (1971) 1917.
[57] A.V. Deshpande, A. Beidoun, A. Penzkofer, G. Wagenblast, Chem. Phys. 142 (1990) 123.
[58] R.G. Kepler, V.S. Valencia, S.J. Jacobs, J.J. McNamara, Synth. Met. 78 (1996) 227.
[59] W. Holzer, A. Penzkofer, R. Stockmann, H. Meysel, H. Liebegott, H.-H. Hörhold, Synth. Met. 125 (2001) 343.
[60] W. Falkenstein, A. Penzkofer, W. Kaiser, Opt. Commun. 27 (1978) 151.
[61] A. Penzkofer, W. Falkenstein, Opt. Quant. Electron. 10 (1978) 399.
[62] V. Kiisk, I. Sildos, A. Suisalu, J. Aarik, Thin Solid Films 400 (2001) 130.
[63] W. Holzer, A. Penzkofer, H.-H. Hörhold, Synth. Met. 113 (2000) 281.
[64] H. Rost, H.-H. Hörhold, W. Kreuzer, H. Spreitzer, Proc. SPIE 3148 (1997) 373.
[65] W. Kreuder, H.-H. hörhold, H. Rost, WO Patent 9709394 A1 (1997), to Hoechst AG, US,48,14244 (1998).
[66] N. Tessler, D.J. Pinner, V. Cleave, P.K.H. Ho, R.H. Friend, G. Yahioghlu, P. Le Barny, J. Gray, M. de Souza, G. Rumbles, Synth. Met. 115 (2000) 57.
[67] S.E. Burns, G. Denton, N. Tessler, M.A. Stevens, F. Cacialli, R.H. Friend, Opt. Mater. 9 (1998) 18.
[68] Y. Kawabe, Ch. Spiegelberg, A. Schülzgen, M.F. Nabor, B. Kippelen, E.A. Mash, P.M. Allemand, M. Kuwata-Gonokami, K. Takeda, N. Peyghambarian, Appl. Phys. Lett. 72 (1998) 141.
[69] S.V. Frolov, M. Shkunov, Z.V. Vardeny, K. Yoshino, Phys. Rev. B 56 (1997) R4363.